NsG-417-61

ThO_2 Dispersion-Strengthened Ni and Ni-Mo Alloys Produced by Selective Reduction

4 pages Code1 Cat 17

by

[redacted]

Jens G. Rasmussen* and Nicholas J. Grant**

ABSTRACT

A series of Ni-ThO_2 and Ni-12Mo-ThO_2 alloys, containing from 3 to 9 volume percent thoria, were prepared by selective hydrogen reduction of mixed submicron oxides. Considerably higher than usual room temperature strength properties with good ductility were obtained. At 932° C, creep-rupture properties were excellent, with significant improvements in strength and stability due to solid solution strengthening of nickel by 12 weight percent molybdenum. Investigated were the benefits derived from additional cold work after hot extrusion, with and without intermediate annealing treatments. An analysis of the probable strain distribution in oxide dispersion-strengthened alloys is presented.

*Formerly Research Assistant, Department of Metallurgy, Massachusetts Institute of Technology, Cambridge, Massachusetts, now in Copenhagen, Denmark.

**Professor, Department of Metallurgy, Massachusetts Institute of Technology, Cambridge, Massachusetts.

Submitted in partial fulfillment of the requirements for the degree of Doctor of Science, Department of Metallurgy, Massachusetts Institute of Technology, Cambridge, Massachusetts, June 1964.

INTRODUCTION

The major efforts to produce oxide dispersion-strengthened alloys, have been concentrated in the past mainly on mechanical mixing and blending methods of metal and oxide powders, on internally oxidized dilute alloys, and on salt decomposition techniques to achieve either the matrix phase, the oxide phase, or both, seeking in each instance, a homogeneous oxide dispersion.

Each of these techniques has its advantages and disadvantages. Mechanical mixing methods demand use of near-micron metal and vastly finer oxide powders; the fine oxides are fairly easy to obtain, whereas the near-micron metal powders are difficult and expensive to produce, especially in alloy form. In internally oxidized alloys, there is the problem of producing uniform, clean fine powders in which the solute element is not already partly oxidized. Further, the amount of oxide which can be incorporated is relatively small, and the variety of alloys, both from the point of view of the metal matrix and the oxide, are of somewhat restricted selection; for example, it is not possible to internally oxidize oxidation resistant alloys containing 10 or more percent chromium.

Salt decomposition techniques, on average, have proven to be quite successful in certain types of alloys, the major problem being one of cost in achieving the desired compositions, especially if decomposable salts are utilized both for the metal matrix and the oxide.

For this program, it was planned to study the feasibility of utilizing mixtures of oxide, followed by selective reduction of the non-refractory oxide or oxides to produce the metal matrix. Most oxides are inexpensive and readily available; are brittle and therefore can be easily comminuted to particles as fine as 0.1 to 0.5 micron; are readily reducible in this fine size, if the free energy of oxide formation is below about 80,000 calories per gram atom of oxygen; and undergo easy alloying with other fine metallic powders which are free of oxide films. Viewing this array of advantages, it was logical to undertake a study of thoria dispersion-strengthened nickel and nickel-12 percent molybdenum alloys. In

mixtures of this sort, both the nickel oxide and molybdenum oxide are readily reducible at temperatures below 1000° C, whereas the thoria is stable well above this temperature. For these alloys, the thoria content varied between 3.5 and 9 volume percent.

There were three major aims to this study:

1. Determine the feasibility of selective reduction from oxide mixtures, as described above to achieve high strength, high temperature alloys.

2. Study the benefits of matrix solid solution strengthening compared to a pure metal matrix.

3. Study the effect of additional cold work beyond that achieved in the extrusion step.

EXPERIMENTAL PROCEDURE

Raw materials. For the nickel thoria and nickel-molybdenum-thoria alloys the raw materials were analytical grade NiO, 98.5 percent pure MoO_2 (balance MoO_3) and thorium nitrate, $[Th(NO_3)_4 \cdot 4H_2O]$. The NiO was in the form of 0.6 micron powder, the MoO_2 was 1 to 5 micron powder, and the thorium nitrate was a liquid solution. The molybdenum oxide was ball milled for about 230 hours, yielding a particle size of 0.5 micron; milling was done in a nickel-lined mill, and resulted in a pick-up of about 17 percent nickel, which became part of the alloy. There resulted formation of about 4 percent metaldehyde through oxidation of ethyl alcohol, the grinding reagent, to acetaldehyde, with subsequent polymerization. This product was removed by vacuum evaporation at 300° C.

One nickel-thoria alloy, N1, was prepared by milling 2 to 5 micron "Inco B" nickel powder in ethyl alcohol. It was observed that thorium nitrate, added to the alcohol in a quantity to produce 7 volume percent of thoria, acted as an excellent ball milling aid, and was utilized in this way in the ball milling operations. The final product, after 360 hours of milling, was 0.5 micron oxidized nickel

powder, intimately mixed with thorium nitrate. The alcohol was removed by vacuum treatment at 80° C.

Decomposition studies. Since it was the intent of this study to produce very fine stable thoria by decomposition of thorium nitrate, preliminary studies were made to estimate the average particle size of thoria as a function of decomposition temperature, time, and atmosphere.

It was found that the logarithm of the average thoria particle size increased linearly with increasing decomposition temperature, the average particle size being only slightly influenced by decomposition conditions other than temperature for times greater than one hour. Decomposition in vacuum resulted in more rapid decomposition than in argon at temperatures below 1000° C. In fact, satisfactory decomposition in vacuum took place as low as 700° C, whereas higher temperatures were necessary for the decomposition step in argon.

Figure 1 shows a plot of average thoria particle size, determined by x-ray line broadening, versus decomposition temperature in vacuum for 1 and 2 hours. This same figure shows the change in weight as a function of time, the loss in weight being attributed to the elimination of water vapor and NO_2 gas, the former accounting for most of the weight change above about 400° C.

Our studies indicate that thorium nitrate decomposition above 600° C results in a thoria crystallite size which is related to time by the following equation:

$$d = K t^{0.1}$$

where d = average thoria crystallite size determined by x-ray line broadening,

t = time in hours

K = average crystallite size after one hour at temperature

Selective oxide reduction. Thermodynamic data from Kubaschewsky and Evans[1] and Elliott and Gleiser[2] clearly showed that it is possible to reduce NiO and MoO_2 in the presence of thoria at temperatures below 1000° C. To

estimate the minimum temperature for reduction of the nickel and molybdenum oxides, and thereby to maintain the finest particle size of thoria, preliminary experiments were made of the selective reduction of mixtures of the three oxides. Precautions were taken to keep the samples protected at all times, since the very fine thoria is hydroscopic, and picks up water readily at the lower temperatures.

Figure 2 shows that most of the oxygen is removed within the first half hour at each temperature, the curve remaining quite flat for longer periods of time. After about 2 hours, each 100° C temperature increment results in an additional weight decrease due to oxygen loss which is close to one-half of the weight decrease for the preceding 100° C temperature increment, or:

$$W_T - W_{T-100} = \frac{1}{2}\left(W_{T-100} - W_{T-200}\right)$$

where W_T = percent weight loss at temperature T. Assuming that the above equation also holds approximately for temperatures above 900° C, one can calculate that the indicated weight loss for essentially complete reduction of alloy powder NM9 is 22.74 percent, and would call for a temperature of 1400° to 1500° C for reduction. Utilizing this figure as the ultimate, one can easily calculate the amount of unreduced oxide at any other temperature for equivalent time. These results are plotted in Figure 3; the curve represents the oxygen content remaining in the alloy.

Alloy production. For alloy production the proper quantities of 0.6 micron NiO, 0.5 micron MoO_2, and thorium nitrate were mixed in a nickel-lined ball mill with ethyl alcohol as the milling liquid. Care was taken throughout the milling operation to be sure that adequate alcohol was added to maintain a suitable viscosity. After 24 hours of milling, the blend was removed from the mill and subjected to an evaporation treatment at 80° C to eliminate the alcohol. The aggregate was then screened to yield a friable aggregate between +20 and -4 mesh, of high porosity.

Batches of 500 grams of the aggregate were vacuum treated in a furnace specifically built to permit detection of the final small weight changes to determine whether all of the water and nitrous oxide had been removed. The vacuum decomposition was carried out at 600° to 700° C for 1 to 3 hours; the results are shown in Table I for the various alloys.

Reduction conditions were also varied among the alloys; some of the earlier alloys were reduced at 600° to 700° C, and at 800° C in later alloys. A constant flow rate of 6 liters of purified hydrogen per minute was utilized for all alloys. Table I summarizes the reduction conditions.

In this table, N designates pure nickel alloys, and NM designates the nickel-12 weight percent molybdenum alloy. After reduction, the powders were cooled in hydrogen to room temperature; care was taken to minimize re-exposure of the product to the atmosphere to avoid water pick-up.

The reduced powders were only about 25 percent dense. Among the earlier alloys, cold compaction was done in a protective argon atmosphere. Either hydrostatic compaction at 35,000 psi, yielding a 50 percent dense product, or hydraulic pressing at 7,000 psi, yielding a density of about 50 percent, was utilized; see Table II.

Compacts through N16 were again vacuum treated after reduction and then treated in hydrogen, both for the purpose of obtaining a small increase in density through sintering and to eliminate any water vapor or oxygen which may have been picked up in the handling of these powders. After alloy N16 the reduced powders were canned and extruded directly, or were compacted in the extrusion can and extruded without further sintering or reduction. Results appeared to be satisfactory, provided that undue delays in processing were avoided.

Hot extrusion was accomplished in mild steel cans which were sealed and evacuated. Extrusion temperatures varied from 954 to 1038° C, with preheat at the same temperatures for 1 to 2 hours. In the case of alloys N17 to NM23 (see

Table II), extrusion was carried out in two steps; the first was a reduction of area of about 4 to 1, and a second at a ratio of 33:1, at each of two different extrusion rates, to achieve final densification and to impart a larger measure of stored energy through deformation. The extrusion conditions are listed in Table II.

As part of the over-all study, efforts were also made to further strengthen some of the alloys by swaging to achieve various degrees of cold work; swaging was done progressively and with intermediate anneals after steps of about 10 percent reduction of area.

Testing and analysis. Table III lists the chemical analyses of the alloys. The higher iron content of alloy N1 is due to the use of a stainless steel mill, whereas a nickel-lined mill was used for all subsequent powder preparation.

Efforts to determine the oxygen content of the alloys after extrusion, by vacuum fusion techniques, were unsuccessful. The thoria reacts with the graphite crucible and is partially reduced, yielding erroneous oxygen values; oxygen values are assumed to be low, based on metallographic studies, but are not known. Carbon and sulfur values are suitably low.

X-ray analysis was made of the nickel-molybdenum alloys to establish the degree to which molybdenum and nickel interdiffuse to give a homogeneous solid solution.

In an effort to determine whether ultrasonic attenuation might yield information regarding the uniformity of the oxide dispersion and the extent of cold work, a Krautkramer USIP10 ultrasonic pulse unit, with a 12 megacycle probe MQ12 was utilized, employing a 10 mm cross-cut quartz crystal. The attenuation values were measured, taking the average attenuation of 5 or more of the multiple echoes from a rod about 5 centimeters long and about 7 to 8 mm diameter. The attenuation was measured directly in decibles (db) on the equipment. As the pulse travelled a round trip for each additional multiple echo, the measured length of the rod was multiplied by 2 when relating results to attenuation per unit length, and is expressed in db/cm. These attenuation values are listed in Table IV.

Room temperature tension tests and creep-rupture tests at 982° C (1800° F) were conducted in air on most of the alloys.

RESULTS

Alloy structure. Unusually uniform oxide dispersions were obtained in most of the alloys, with very little stringering, particularly in the nickel-molybdenum-thoria alloys. Figure 4 shows the structure of alloy NM23, longitudinal section, 1000X. In Figure 5, an electron micrograph of alloy NM15 at 10,000X, using a carbon replica technique, is shown in a longitudinal section. On the other hand alloy N1, which shows a stringered structure (see Figure 6), otherwise shows good oxide distribution and properties were quite good. Alloy N1 was prepared from metallic nickel instead of NiO.

The average particle size of the thoria phase, achieved by electrolytic extraction, and using x-ray line broadening techniques, is shown in Table V. The oxides were extracted by dissolving alloy chips in hot nitric acid.

Room temperature mechanical properties. Table VI lists the room temperature values of 0.2 percent yield strength, ultimate tension strength, elongation, reduction of area, and hardness for the nickel-thoria and nickel-molybdenum-thoria alloys. It is fairly obvious that strength increases with increasing thoria content, on average, and ductility decreases. Correspondingly, hardness increases with increasing thoria content. There are several deviations from this behavior primarily in the nickel-thoria alloys, which show the best strength and ductility combination in the 7 volume percent thoria alloys. These deviations are directly associated with both the perfection of the oxide dispersion, and the amount of stored energy as a result of the extrusion step.

It is worth noting that these room temperature mechanical properties are the best (by a considerable margin) reported to date, both for oxide dispersion-strengthened nickel alloys, and for nickel-molybdenum alloys with a thoria dispersion.

Creep-rupture tests at 982° C (1800° F). Figures 7 and 8 are plots of log stress versus log rupture time for nickel-thoria and for nickel-molybdenum-thoria alloys, respectively.

It is observed that the nickel-thoria alloys all undergo an instability break in the curves with the exception of N17, Figure 7. In contrast, the Ni-Mo-thoria alloys do not show instability breaks in tests which lasted even more than 100 hours.

Further cold work. To determine the benefits which might be gained through additional cold work of the as-extruded alloys, room temperature swaging was done on a number of the alloys in two different series. Nickel-thoria and one nickel-molybdenum-thoria alloy were swaged progressively to larger reductions without intermediate anneals; similarly, the same or comparable alloys were cold worked with intermediate anneals between each reduction of about 10 percent. In the former case the alloys were N1, N16, and NM15; in the latter case they were alloys N16 and NM15, with intermediate anneals of one hour at 950° and 700° C, respectively. The temperature of 700° C is below the recrystallization temperature of the nickel-molybdenum alloy (3), and would correspond to a polygonization type treatment; 950° C is above the recrystallization temperature of pure nickel, and would correspond, for this alloy to a treatment more nearby approaching, complete recovery.

Figure 9 shows the increase in rupture life for the swaged alloys, with and without intermediate annealing treatments, all tests, in air were at 982° C at the indicated stresses. Alloys N1 and N16 each show a plateau in the rupture life curve with increasing reduction of area by swaging. N16, with 5 percent thoria, shows an increase of about 17:1 in rupture life compared to the as-extruded condition, whereas alloy N1 and 7 percent thoria shows only a very small increase.

Alloy N16 showed a more rapid rate increase in rupture life up to almost 30 percent reduction of area when utilizing intermittent anneals, but reached a plateau sooner than without intermediate anneals.

It is interesting to observe that alloys N1 and N16 showed first cracks when reduction of area values by progressive swaging were 42 and 63 percent, respectively; with intermittent anneals, alloy N16 did not show any signs of cracking at 51 percent reduction of area, this being the highest value attempted in the current program.

Alloy NM15 not only shows a more rapid rise in rupture life with cold swaging, but did not strike a plateau after a considerable increase in rupture life. The rate of rise was greater with intermittent anneals than with progressive reductions without annealing, and in each case the tests were extended only to the point where a strengthening factor of about 35:1 was achieved for each condition, this value being about 20 percent reduction of area for NM15 with intermittent anneals, and about 33 percent for the same alloy without intermittent anneals. In each case, the next increment of cold work did result in first cracks; this occurred at 28 percent reduction for annealed NM15, and at 42 percent without annealing.

For NM15 this increase in rupture time corresponds to an increased load carrying capacity of about 2,000 psi for a 100-hour life at 982° C (1800° F); this is an increase from about 7,000 to 9,000 psi for a 100-hour life (see Figure 8).

A study of the change in hardness with progressive cold reduction by swaging (see Table VII), shows that the first 10 percent cold reduction decreased the as-extruded hardness by a significant amount. It required 45 percent reduction of area in the case of alloy N1 to regain the as-extruded hardness, and required about 33 percent reduction of area in the case of N16. Intermittent anneals, in the case of alloy N16 bring about a return to the as-extruded hardness after a total reduction of area of about 17 percent following an anneal after 7 percent reduction of area. After this the hardness remains essentially constant out to 52 percent reduction of area.

Alloy NM15 at first shows a small decrease in hardness followed by an increase in hardness over that of the as-extruded condition, for a net increase of about 20 Vickers hardness points after 42 percent reduction of area through progressive

cold work. Intermittent anneals between the various reduction of area steps result in a small continuing decrease in hardness, for a net loss of almost 10 points after about 27 percent reduction of area.

The ultrasonic attenuation tests also indicate that there is a parallel rise in values of log attenuation versus reduction of area by cold swaging, paralleling to a major degree the increase in rupture life with increasing cold swaging. These results can be checked from Table IV. In particular, the parallel increase for alloy NM16 with intermittent anneals of log attenuation and rupture life with increasing cold work is quite striking, although at the moment not totally explainable.

X-ray diffraction studies. Texture and line broadening studies were undertaken using a pin-hole back reflection camera with a distance of 5 centimeters between specimen and film, utilizing filtered CuK_α radiation.

In the as-extruded condition, the nickel-molybdenum-thoria alloys showed virtually no texture, confirming the observed microstructures. The nickel-thoria alloys showed a mild <100> wire texture, plus a smaller amount of <111> wire texture, in agreement with the findings of Tracey and Worn on Ni-ThO_2 alloys[4].

Larger extrusion ratios produced a more pronounced texture in the nickel-thoria alloys, but did not appear to develop a significant texture in the nickel-molybdenum-thoria alloys.

Variations in cold swaging, with and without intermittent annealing treatments, did bring about small changes in texture. Alloy NM18, twice extruded, did develop a small amount of <100> wire texture. Increased swaging with intermittent annealing of alloy NM15 also produced a small amount of <111> wire texture. On the other hand, the nickel-thoria alloys developed a strong <111> wire texture with increased swaging and intermittent annealing treatments at 950° C. Without the intermittent anneals, the texture developed was predominantly the <100> wire texture.

In the as-extruded condition, all of the alloys in this investigation showed sharp reflections with well separated $K_{\alpha I}$ and $K_{\alpha II}$ (331) and (420) lines in the back-reflection patterns. Swaging without annealing of the nickel-molybdenum-thoria alloys resulted in pronounced line broadening. The nickel-thoria alloys, on the other hand, showed only a small increase in line width for similar treatments. Annealing of the swaged alloys resulted in a return to the original line width in the case of the nickel alloys and a partial return in the case of the Ni-Mo alloys.

Figure 10 shows the changes in back-reflection patterns for alloys NM15 and N16 following a 25 percent reduction of area by cold swaging, and also after subsequent annealing for one hour at 950° C for NM15 and 700° C for N16.

DISCUSSION

Structure and properties. It is evident, both from metallographic studies and x-ray diffraction analysis that nickel-thoria and nickel-molybdenum-thoria alloys with uniform oxide dispersion and excellent low and high temperature properties can be produced by selective oxide reduction from a mixture of oxides. The starting oxides can be readily comminuted to sub-micron particle size (about 0.5 micron in this instance), allowing for easy alloying of the reduced nickel and molybdenum powders, and leading to a fine oxide dispersion in which the oxide particle size varies between 100 and 390 Å diameter. The resultant thoria particle size was somewhat smaller than had been anticipated from preliminary experiments, due in part to the formation of very thin layers of thoria on the nickel and molybdenum oxides. Apparently these coatings are relatively adherent and porous. The effectiveness of the thoria coating is suggested by the lack of sintering at very high temperatures after complete reduction of the nickel and molybdenum oxides. If one assumes a mixture of 0.5 micron metallic particles with a uniform coating of thoria to yield 7 volume percent of oxide, this would indicate a coating thickness of about 60 Å.

Because of the fineness of the oxide dispersion and its uniformity, and because of the homogeneity nature of the resultant nickel-molybdenum solid solution, good properties were achieved in this oxide dispersion-strengthened alloy.

In plots of log stress versus log rupture time for nickel-thoria alloys tested at 982° C, the instability breaks which were observed in all of the alloys except the 3.5 volume percent thoria alloy are not understood. It is possible that there was a slight amount of reoxidation of the nickel powder, due primarily to water pick up by the fine hydroscopic thoria. This does not, however, explain the absence of an instability break in the 3.5 percent thoria alloy (except that this low thoria content resulted in a smaller water vapor pick up and less reoxidation). In view of the resultant fine thoria particle size, it should be possible to use a higher temperature vacuum reduction treatment of the compact to protect against water vapor pick-up by the thoria.

The nickel-molybdenum-thoria alloys did not show an instability break at 982° C for rupture times of more than 100 hours. It is possible that the much slower diffusion rates of oxygen in the nickel-molybdenum matrix may have resulted in a more stable alloy. The more flat slopes of the curves in Figure 8 compared to Figure 7 would suggest a more stable alloy system generally.

The nickel-molybdenum-thoria alloys are considerably stronger than the nickel-thoria alloys made by the same techniques, indicating important benefits to be derived from strengthening of the matrix through alloying. These Ni-Mo alloys are, however, not stronger than Ni-ThO_2 alloys made by other techniques by a small amount[4,5,6].

Elongation values in the 982° C stress-rupture tests were from 2 to 5 percent for the as-extruded alloys and from 3 to 7 percent for the cold worked and annealed alloys. These ductility values compare well with reported values in the literature[4,5,6].

The high 982° C strength properties are matched by significantly stronger tension values at room temperature. Compared to the nickel-thoria alloys, the ductilities are slightly less and the hardness values are significantly higher for the nickel-molybdenum-thoria alloys (see Tables VI and VII).

As was expected, the room temperature strength generally increased with increasing thoria content, and ductility decreased. Alloy NM15 with a yield strength of 162,000 psi and ductility values of 2.8 percent elongation and 11.4 percent reduction of area was able to withstand about 40 percent additional cold reduction by swaging before cracking. Similarly, alloy N16 with 141,700 psi yield strength, and 145,000 psi ultimate tension strength, 7.8 percent elongation and 36.1 percent reduction of area, withstood 63 percent reduction of area by cold swaging before cracking slightly. Still higher strength values were obtained by some of the higher thoria content alloys, but ductilities were sufficiently lower than they would probably have withstood considerably smaller amounts of additional cold reduction before cracking.

On average, the room temperature strength values of these alloys are very much greater than values reported previously for comparable oxide dispersion-strengthened metals made by many techniques[4,5,6] including some which were similar to the techniques used in this work.

Effects of additional cold work by swaging. The results of this study, as well as from the work of Tracey and Worn[4] indicate that deformation at room temperature of oxide dispersion-strengthened alloys can improve the high temperature creep-rupture properties. The mechanism of this increase in strength is not well understood. It is clear that a significant but unknown amount of cold work is retained by the alloys during the hot extrusion step. The quantity of stored energy is a function of the reduction ratio in the extrusion step, the oxide content, and the rate and temperature at which the extrusion takes place. Due to variations in interparticle spacing and particle size of the oxide, the quantity of retained energy in extrusion is seldom known in more than an approximate way.

Stored energy of deformation can be achieved by a high strain rate - high temperature deformation process, or the energy can be added later by deformation at lower temperatures, for example, at room temperature. For most effective retention of stored energy, one should first have a completely dense body, and avoid transformations either of the oxide or of the metal, which might result in volume changes and thereby in a disturbance of the stored energy distribution.

In order to determine whether significant improvements might be achieved by increasing the reduction ratio, alloys N17 and NM18 were produced by a two-step extrusion process (see Table II). The first extrusion took place at a ratio of about 4:1, leading to a density of 99.5 percent for alloy N17 and 98.6 percent for alloy NM18. Each alloy was then re-extruded at the same temperature at an extrusion ratio of about 33:1, leading to a density of 99.3 percent for alloy N17, and 99.0 percent for alloy NM18. These 3.5 volume percent thoria alloys did not appear to be effectively strengthened by the additional much higher extrusion reduction relative to the higher oxide containing alloys, with the puzzling exception that alloy N17 is the only one of the nickel-thoria alloys which did not show an instability break at 982° C (1800° F).

To determine the effect of the rate of extrusion, alloys N19 and 20 and NM22 and 23, all with about 9 percent ThO_2, were extruded first at an extrusion ratio of about 4.5 to 1 for consolidation. All four alloys were then re-extruded at 1038° C at a ratio of 33 to 1, with alloys N20 and NM22 extruded at a slow rate (ram speed 43 inches per minute) and N19 and NM23 at a high rate (145 inches per minute). As observed in Figures 7 and 8, the higher strain rate extrusions resulted in stronger alloys, supporting the observation that higher strain rate deformation results in higher stored energy and higher strength at elevated temperatures.

The response of these alloys to some of the processing variables is complex. One of the behavior patterns more difficult to explain is the difference in response to cold work by the Ni alloys compared to the Ni-Mo alloys. The much better

microstructure of the NM alloys and their lack of a preferred texture in the as-extruded condition probably explain most of the differences. The NM alloys, even with extensive cold work did not develop a strong texture; they did not soften nearly as much with additional cold work (change in direction of cold work was involved), and retained the cold work after annealing. In contrast, the N alloys showed a preferred texture, which became worse with further cold work, and underwent significant softening with increased cold swaging. Finally, the N alloys seemed to recover much more easily than the NM alloys due to annealing.

Mechanism of strengthening. Evidence has been advanced by several investigators that the source of strength in oxide dispersion-strengthened alloys is the stored energy of deformation of equivalent cold work. The function served by the oxide is then to hinder or delay recovery and recrystallization process[7]. The presence of strain fields around fine particles has been demonstrated by Thomas and Nutting[8].

Motion of dislocations through an array of fine oxide particles dispersed on a sub-micron scale is made more difficult by the volume of the strain field due to cold work around the particles, in effect decreasing the particle spacing and increasing the resistance to metal flow.

The above is a simple picture of an oxide dispersion-strengthened alloy, but it fails to explain the increase in ductility of these alloys with further cold work when intermediate anneals are used; these annealing treatments are quite low, for example, at 400° to 700° C for a nickel matrix. At these low temperatures, only recovery (probably polygonization) occurs. Whereas Clarebrough et al[9] show that stored energy release has a recrystallization peak at 550° C for pure nickel, and total energy release at about 650° C, this study shows that cold worked Ni-ThO_2 annealed at 700° C shows sharpening of diffraction rings and Ni-Mo-ThO_2 shows a similar effect at 950° C (see Figure 10), without recrystallization.

It is probable that the alloy behaves as a simple two phase structure: the matrix metal between particles which behaves more or less like the pure metal, responding to cold work and annealing treatments normally but with temperature and time delays; and the matrix metal around the oxide particles, which contains extensive dislocation tangles.

Figure 11 suggests a possible model of the structure, starting in each case with an as-extruded (hot) structure which has a relatively high level of stored energy. The level of stored energy, relative to the fracture stress, σ_F, is unknown, and depends on the following:

a) interparticle spacing (stored energy is retained at elevated temperatures when the spacing is about 1 micron or less),

b) volume content of oxide (even oxide clusters are important in storing energy of deformation),

c) extrusion ratio and extrusion rate at the extrusion temperature.

Figure 11 (A, B, C) suggests that with progressive cold work a high total content of energy is stored, with the matrix metal highly strained. The effective, interparticle spacing, IPS', decreased rapidly with cold work, however, at some level of cold work, the fracture stress is exceeded locally and cracking occurs during rolling. In contrast, if intermediate anneals are utilized, the matrix between particles recovers through polygonization[10], leaving a low level of stored energy. The dislocation tangles around the oxide particles are not eliminated by these low temperature anneals, and in fact, are resistant to complete recovery even at very high temperatures[6, 10, 11, 12]. The recovered matrix is now able to undergo significant additional strain (ductility improves) while the decrease in effective interparticle spacing brings about an improvement in strength over the as-extruded condition.

If one starts with a lower level of total strain energy in the as-extruded state (low extrusion ratio and low extrusion rate at high temperatures), considerably more stored energy can be added through subsequent cold work, probably with a more advantageous distribution of strain energy if intermediate low temperature anneals are utilized. Similarly, lower oxide content and more perfect oxide distribution will permit greater improvement through alternate cold working and annealing of the as-extruded structure. Oxide clusters in a structure otherwise possessing uniform particle distribution may be associated with good as-extruded properties but will suffer from low ductility and will crack after small amounts of additional cold work. This happens because the clusters permit the fracture stress to be exceeded in the matrix metal between the extremely closely spaced oxide particles in the cluster.

CONCLUSIONS

1. Using mixtures of sub-micron oxides of NiO and ThO_2 and NiO, MoO_2, and ThO_2, the thoria derived from thorium nitrate decomposition, and followed by selective reduction of the NiO and MoO_2, high levels of room temperature strength and 982° C creep-rupture strength were achieved.

2. Alloying of the reduced sub-micron nickel and molybdenum was complete during hot extrusion.

3. The Ni-Mo-ThO_2 alloys did not show any structural instabilities in 982° C creep-rupture tests for test times up to 100 hours. Most of the Ni-ThO_2 alloys showed an instability break.

4. Cold work, with and without intermediate low temperature annealing treatments, was effective in increasing the 982° C strength; and was more effective in the Ni-Mo alloys than in pure nickel, and more effective with intermediate annealing treatments.

5. A model is proposed to indicate the possible distribution of stored energy for oxide dispersion-strengthened alloys which are cold worked after extrusion, with and without intermediate, low temperature annealing treatments.

ACKNOWLEDGEMENTS

The authors are indebted to NASA for support of the program under contract NsG-117-61. Thanks are expressed to Krautkrämer Ultrasonics, Inc. for loan of equipment and discussions to measure ultrasonic attenuation.

REFERENCES

1. Kubaschewsky, O. and Evans, E.L.: "Metallurgical Thermochemistry", Pergamon Press, Oxford, (1958).

2. Elliott, J.F. and Gleiser, M.: "Thermochemistry for Steelmaking", Reading, Mass., 1, Addison-Wesley Publ., (1960).

3. Belloux, R. and Grant, N.J.: "Solid Solution and Second-Phase Strengthening Nickel Alloys at High Temperatures", Trans. AIME Met. Soc., 218, (1960), 232.

4. Worn, D.K. and Tracey, V.A.: "Powder Metallurgy" (Symposium on "Non-Metallic Dispersions in Powder Metallurgy"), (1962), 34.

5. Murphy, R. and Grant, N.J.: "Powder Metallurgy" (Symposium on Non-Metallic Dispersions in Powder Metallurgy), 1, (1962).

6. Predecki, P, and Grant, N.J.: "Oxide Refractoriness in Dispersion-Strengthened Copper and Nickel Alloys", Proc. ASTM, 63, (1962).

7. Grant, N.J.: "A Look at Dispersion-Strengthening by Powder Metallurgy Methods". Progress in Powder Metallurgy, 16, Capitol City Press, Montpelier, Vt., (1960).

8. Thomas, G. and Nutting, J.: "The Plastic Deformation of Aged Aluminum Alloys", with Appendix by P.B. Hirsch, J. Inst. Metals, 86, 7, (1957).

9. Clarebrough, H.M., Hargreaves, M.E. and West, G.W.: "The Release of Energy During Annealing of Deformed Metals", Proc., Royal Soc., (London), 232A, (1955), 252.

10. Komatsu, N. and Grant, N.J. "Thermal Stability of Cu-SiO_2 and Cu-Al_2O_3 Alloys". Trans. AIME Met. Soc., 224, (1962), 705.

11. Bonis, L. and Grant, N.J.: "The Structure and Properties of Dispersion-Strengthened Internally Oxidized Alloys". Trans. AIME Met. Soc., 224, (1962), 308.

12. Bonis, L. and Grant, N.J.: "Influence of Processing Variables on the Properties of Ni-Al_2O_3 Alloys". Trans. AIME, 218, (1960), 877.

TABLE I

Decomposition and Hydrogen Reduction Data for Alloy Powders

Alloy No.	Nominal Composition*	Decomposition Time and Temp. ° C	Reduction Time and Temp. ° C	Heat Treatment of Compact Time and Temp. ° C
N1+	Ni-7 ThO_2	1h-600 1h-700	5h-600 2h-700	2h-600-vac. 1h-800-vac. 4h-800-H_2
NM9(I)	Ni-Mo-7 ThO_2	1h-600	23h-600	1.5h-600-vac. 14h-600-H_2
NM9(II)	Ni-Mo-7 ThO_2	1h-600	11h-800	3h-600-vac. 1h-800-vac. 9h-600-H_2 2h-800-H_2
N10(III)	Ni-7 ThO_2	1h-600	23h-600	1.5h-600-vac. 14h-600-H_2
N10(IV)	Ni-7 ThO_2	1h-600	13h-800	3h-600-vac. 1h-800-vac. 11h-600-H_2 2h-800-H_2
NM15	Ni-Mo-5 ThO_2	1h-600	14h-800	5h-600-vac. 1h-800-vac. 12h-800-H_2
N16	Ni-5 ThO_2	1h-600	11h-800	5h-600-vac. 1h-800-vac. 12h-800-H_2

TABLE I (cont'd.)

Decomposition and Hydrogen Reduction Data for Alloy Powders

Alloy No.	Nominal Composition*	Decomposition Time and Temp. ° C	Reduction Time and Temp. ° C	Heat Treatment of Compact Time and Temp. ° C
N17	Ni-3.5 ThO_2	2.5h-600 1h-700	18h-800	None. Extruded as uncompacted powder.
NM18	Ni-Mo-3.5 ThO_2	2h-600 1h-700	10h-800	None. Extruded as uncompacted powder.
N19-20	Ni-9 ThO_2	2h-600 1h-700	8h-800	None. Compacted in extrusion can.
NM22-23	Ni-Mo-9 ThO_2	2h-600 1h-700	6.5h-800	None. Compacted in extrusion can.

+Made using elemental nickel.

*Mo content is 12 weight percent in Ni-Mo alloys, and ThO_2 is in volume percent.

TABLE II

Summary Extrusion

Alloy No.	Nominal Composition*	Compacting Method	Density of Compact %	Preheating Time and Temp ° C	Nominal Extrusion Ratio	Ram Speed Inches per Minute	Density % of Theoretical
N1	Ni-7 ThO_2	Hydrostat. 35,000 psi	62.5	1h-954	23:1	42	99.4
NM9(I)	Ni-Mo-7 ThO_2	Hydrostat. 35,000 psi	56.6	1h-1038	12:1	42	99.5
NM9(II)	Ni-Mo-7 ThO_2	Hydrostat. 35,000 psi	61.4	1h-1033	12:1	42	99.7
N10(III)	Ni-7 ThO_2	Hydrostat. 35,000 psi	53.8	1h-1033	12:1	42	96.9
N10(IV)	Ni-7 ThO_2	Hydrostat. 35,000 psi	50.8	1h-1033	12:1	42	98.8
NM15	Ni-Mo-5 ThO_2	Hydrostat. 35,000 psi	64.2	1h-1033	23:1	42	99.3
N16	Ni-5 ThO_2	Hydrostat. 35,000 psi	62.3	1h-954	23:1	42	99.8
N17	Ni-3.5 ThO_2	Ext. as loose powder	25.0	2h-982	4.5:1 **	40	95.7
	Ni-3.5 ThO_2	Re-extrusion	95.7	2h-982	33:1	40	99.3
NM18	Ni-Mo-3.5 ThO_2	Ext. as loose powder	25.5	2h-1038	4.5:1 **	40	98.6
	Ni-Mo-3.5 ThO_2	Re-extrusion	93.6	2h-1038	33:1	40	99.0

TABLE II (cont'd.)

Summary Extrusion

Alloy No.	Nominal Composition*	Compacting Method	Density of Compact %	Preheating Time and Temp ° C	Nominal Extrusion Ratio		Ram Speed Inches per Minute	Density % of Theoretical
N19-20	Ni-9 ThO_2	Compacted in extrusion can 7,000 psi	43.2	2h-982	4:1	**	43	not deter.
N19	Ni-9 ThO_2	Re-extrusion	?	2h-982	33:1		145	98.5
N20	Ni-9 ThO_2	Re-extrusion	?	2h-982	33:1		43	98.8
NM22-23	Ni-Mo-9 ThO_2	Compacted in extrusion can 7,000 psi	51.8	2h-1033	4:1	**	43	not deter.
NM22	Ni-Mo-9 ThO_2	Re-extrusion	?	2h-982	33:1		43	99.6
NM23	Ni-Mo-9 ThO_2	Re-extrusion	?	2h-982	33:1		145	99.8

*Mo content is 12 weight percent in Ni-Mo alloys; ThO_2 content is volume percent.

**Represents a first extrusion at about 4:1 for densification, followed by re-extrusion of portions at higher extrusion ratios and two extrusion rates.

TABLE III

Chemical Composition of Alloys

Alloy No.	Molybdenum Weight %	ThO_2 Volume %	Impurities, Weight %		
			Fe	C	S
N1	-	6.96	0.29	0.007	0.001
NM9(I)	12.58	6.57	-	-	0.007
NM9(II)	12.41	6.45	-	-	0.005
N10(III)	-	6.41	-	-	0.007
N10(IV)	-	5.95	-	-	0.003
NM15	12.0	4.44	0.062	0.008	0.004
N16	-	4.60	0.043	0.005	0.002
N17	-	3.16	0.025	0.020	-
NM18	11.46	3.22	0.055	0.015	-
N19	-	8.33	0.013	0.011	- *
N20	-	8.32	0.014	0.009	- *
NM22	12.37	8.35	0.016	0.009	- *
NM23	12.54	8.23	0.015	0.006	- *

*From same starting compact; analyses indicate reproducibility of results.

TABLE IV

Ultrasonic Attenuation at 12 mc

Alloy No.	Condition of Sample	Attenuation db/cm
NM15	As extruded	0.81
NM15	Heated 1 hour at 950° C	1.29
NM15	Swaged 33% + 1 hour 950° C	1.50
N16	Swaged 33%	0.39
N16	Swaged 43%	0.46
N16	Swaged 49%	0.45
N16	Swaged 56%	0.71
N16	Swaged 56% + 1 hour 700° C	0.71
N17	As extruded	0.30
N17	Heated 1 hour 700° C	0.31
NM18	As extruded	0.24
NM18	Heated 1 hour 950° C	0.41
	The following two alloys were swaged with intermittent anneals, NM15 1 hour at 700° C and N16 1 hour at 950° C.	
NM15	Swaged 15%	1.35
NM15	Swaged 19%	1.38
NM15	Swaged 28%	1.77
N16	Swaged 17%	0.37
N16	Swaged 35%	0.35
N16	Swaged 42%	0.44
N16	Swaged 51%	0.66

TABLE V

Average Particle Size of Extracted ThO_2

Alloy No.	Average Particle Size Angstroms	
N1	150	
NM9(I)	230	
NM9(II)	260	
N10(III)	310	
N10(IV)	240	
NM15	290	
N16	180	
N17	250	
NM18	280	
N19	290	*
N20	300	*
NM22	360	•
NM23	390	•

*From same starting compact

TABLE VI

Room Temperature Mechanical Properties

Alloy No.	Nominal Composition ThO_2 in Vol. %	U.T.S., psi	0.2% Y.S., psi	El. %	R.A. %	Hardness Vickers 1 kg load kg/mm^2	Hardness Rockwell C
			A. Nickel Alloys				
N17	3.5 ThO_2	86,200	74,900	21.5	67.6	266	25
N16	5 ThO_2	145,300	141,700	7.8	36.1	296	31
N10(III)	7 ThO_2	124,700	123,700	2.5	7.5	257	24
N10(IV)	7 ThO_2	155,900	151,100	3.2	12.3	279	29
N1	7 ThO_2	152,700	146,000	2.3	11.8	334	34
N19	9 ThO_2	131,700	128,800	3.0	1.5	334	30
N20	9 ThO_2	139,700	135,100	2.8	8.2	334	30
			B. Nickel-Molybdenum Alloys				
NM18	3.5 ThO_2	148,800	146,900	11.7	18.8	384	38
NM15	5 ThO_2	167,400	162,000	2.8	11.4	380	37
NM9(I)	7 ThO_2	207,600	200,900	1.9	4.1	432	43
NM9(II)	7 ThO_2	175,600	(175,600)	nil	nil	401	40
NM22	9 ThO_2	194,400	188,100	0.9	4.6	407	33
NM23	9 ThO_2	195,300	193,500	0.9	2.0	407	33

TABLE VII

Hardness Values for Cold Swaged Alloys With and Without Intermediate Annealing

Without Annealing			With Intermediate Annealing		
Alloy	Condition	Vickers Hardness kg/mm^2	Alloy	Condition	Vickers Hardness kg/mm^2
N16	As extruded	296	N16*	7% reduction	277
	7% reduction	277		17% reduction (A)	296
	26% reduction	286		35% reduction (A)	290
	33% reduction	293		42% reduction (A)	285
	51% reduction	292		51% reduction (A)	289
	62% reduction	291			
N1	As extruded	334			
	8% reduction	313			
	18% reduction	315			
	35% reduction	318			
	43% reduction	325			
	47% reduction	329			

TABLE VII (cont'd.)

Hardness Values for Cold Swaged Alloys With and Without Intermediate Annealing

Without Annealing			With Intermediate Annealing		
Alloy	Condition	Vickers Hardness kg/mm^2	Alloy	Condition	Vickers Hardness kg/mm^2
NM15	As extruded	380	NM15**	6% reduction	378
	6% reduction	378		15% reduction (A)	375
	25% reduction	395		18% reduction (A)	377
	33% reduction	399		24% reduction (A)	372
	42% reduction	400		27% reduction (A)	373

*1 hour at 950° C

**1 hour at 700° C

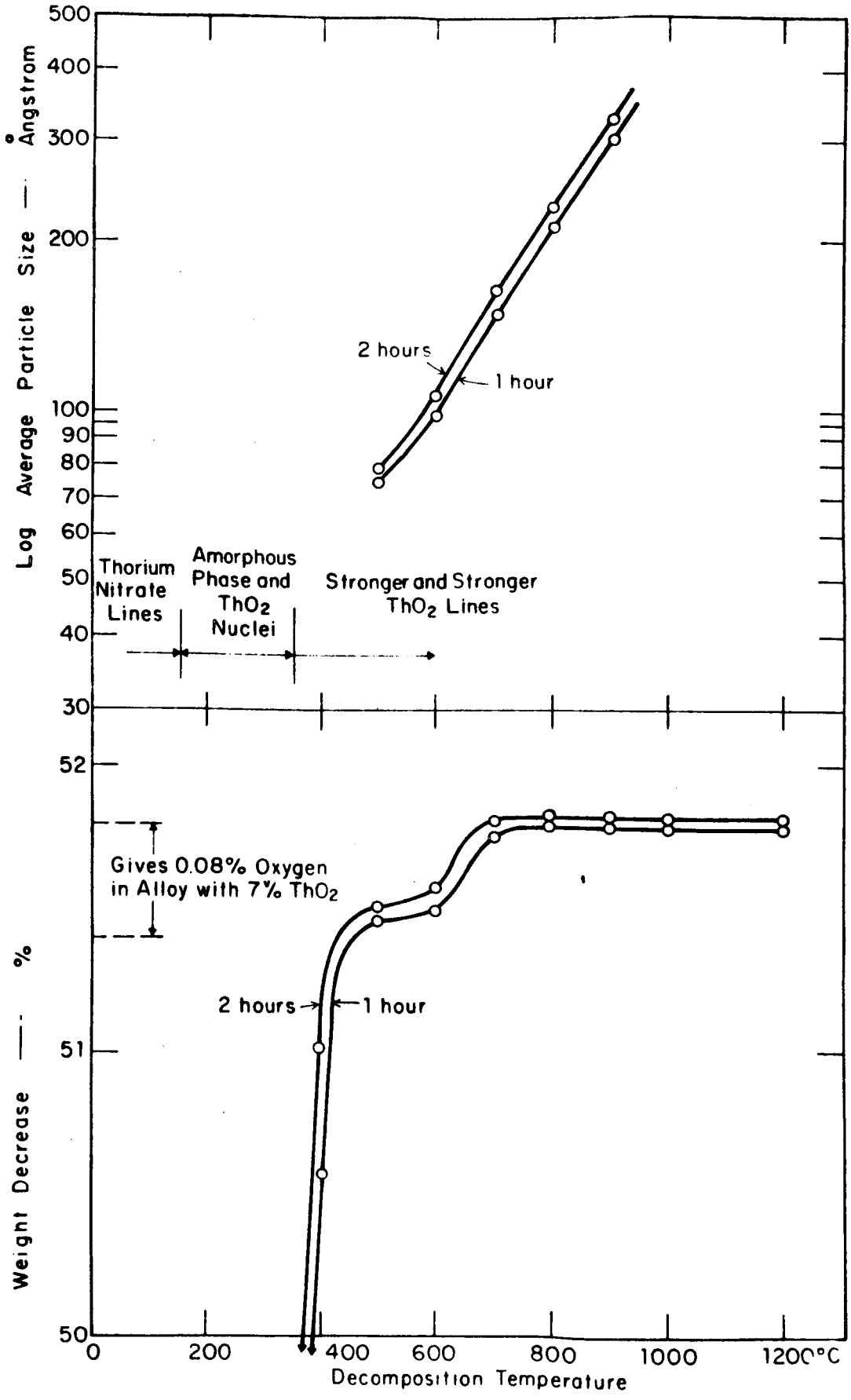

Figure 1. Average thoria particle size and weight decrease as a function of decomposition temperature for 1 and 2 hour periods, for thorium nitrate treated in vacuum.

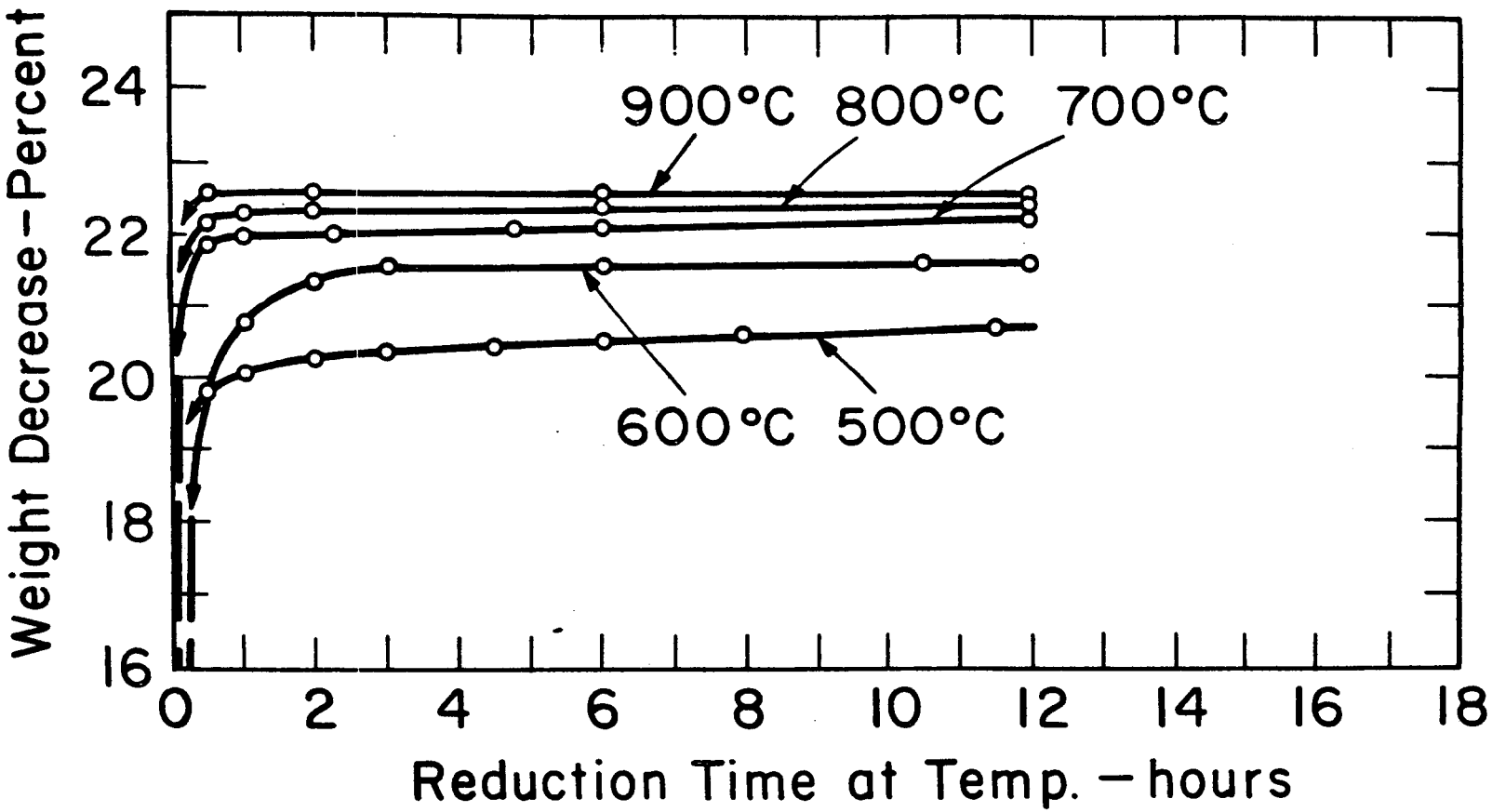

FIG. 2

Weight loss for alloy NM9 powder reduced in hydrogen at flow rate of 2 liters per minute.

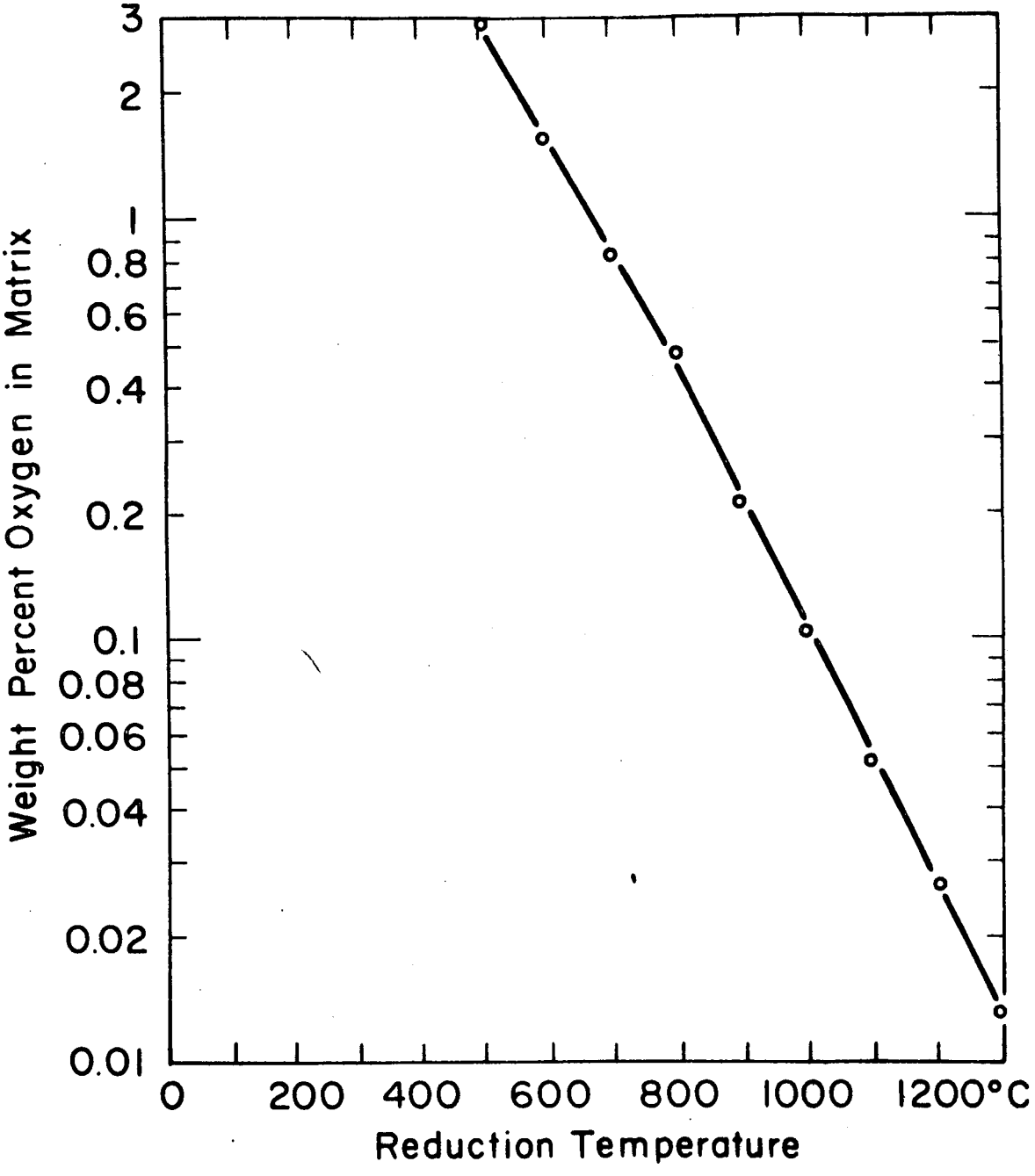

FIG. 3

Weight percent oxygen in alloy matrix as a function of unreduced oxide (other than thoria).

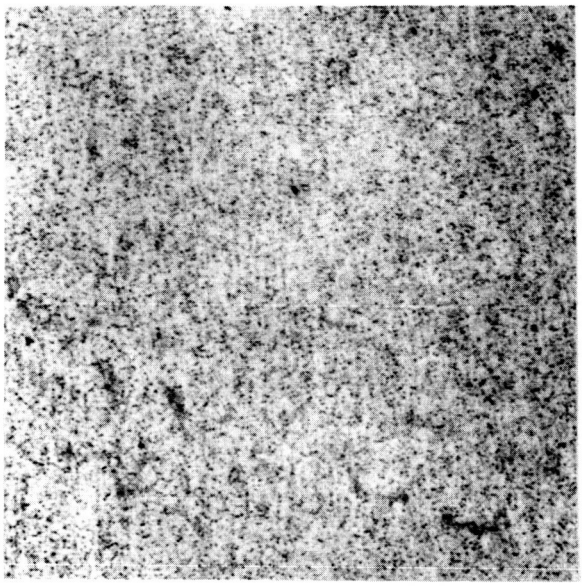

Fig. 4 Alloy NM23 (Ni-12Mo-7ThO_2), longitudinal view. As-extruded. Electrolytic etch, 5% HCl plus alcohol. X 1000.

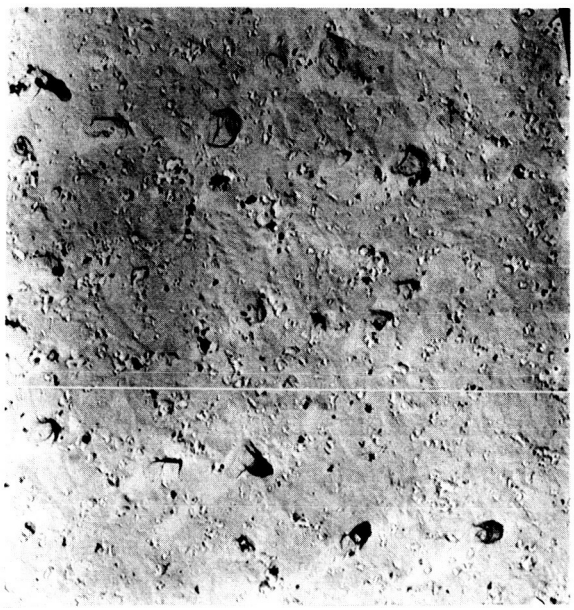

Fig. 5 Alloy NM15 (Ni-12Mo-5ThO_2), longitudinal view. As-extruded. Light electrolytic etch, 5% HCl plus alcohol. X 10,000.

Fig. 6 Alloy N1 ($Ni-7ThO_2$, using elemental nickel), longitudinal view. As-extruded. Electrolytic etch, 5% HCl plus alcohol. X 1000

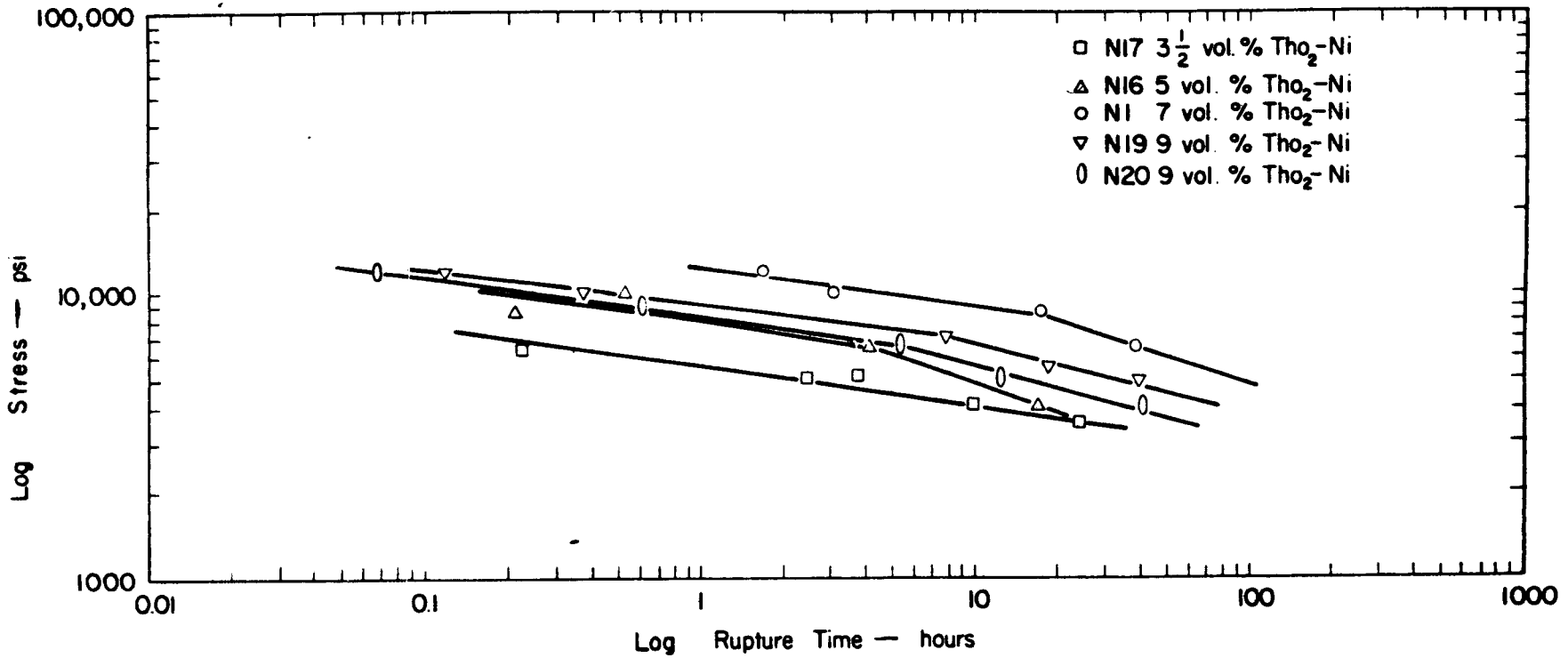

Figure 7. Log stress vs. log rupture time for tests of Ni-ThO_2 alloys, in air, at 982° C (1800° F).

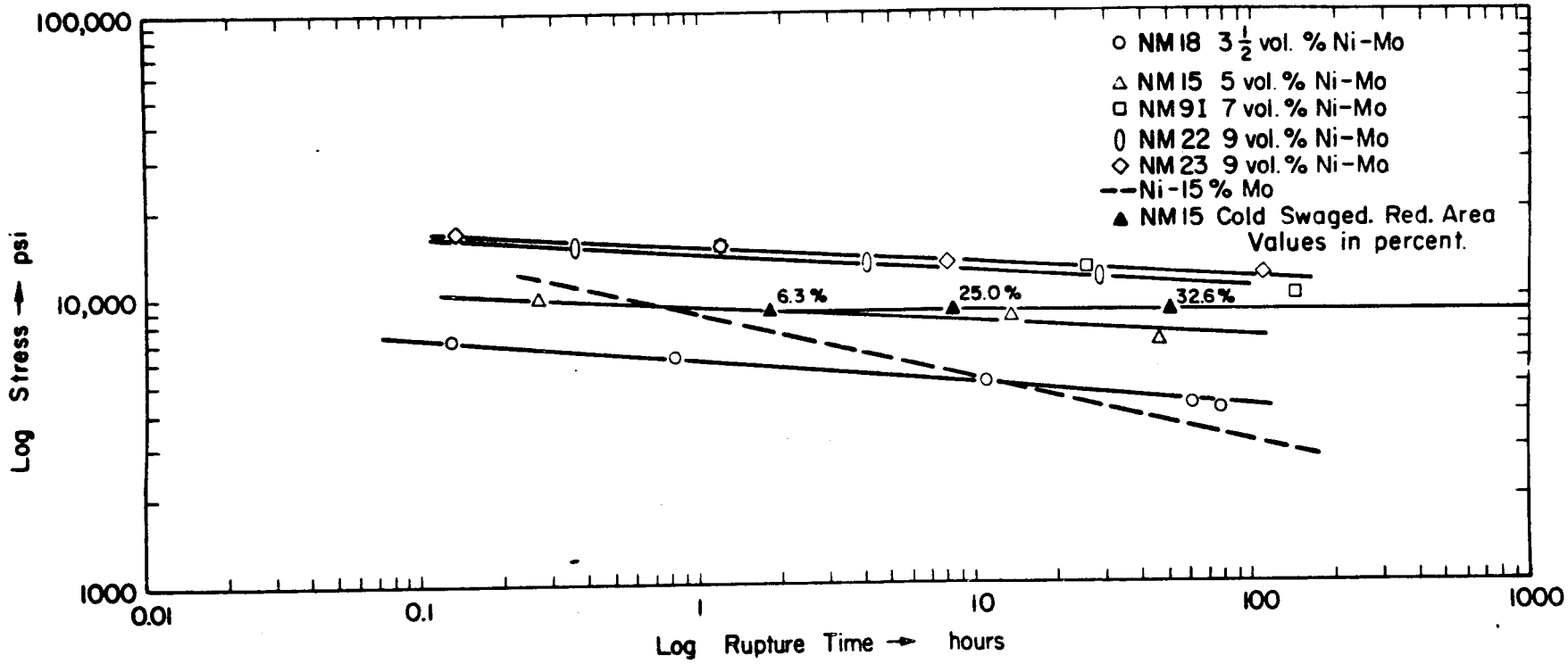

FIG. 8

Log stress vs. log rupture time for tests of Ni-Mo-ThO_2 in air, at 932° C (1800° F). Solid triangles show increase in rupture life with increasing cold work for NM15, tested at 9,000 psi.

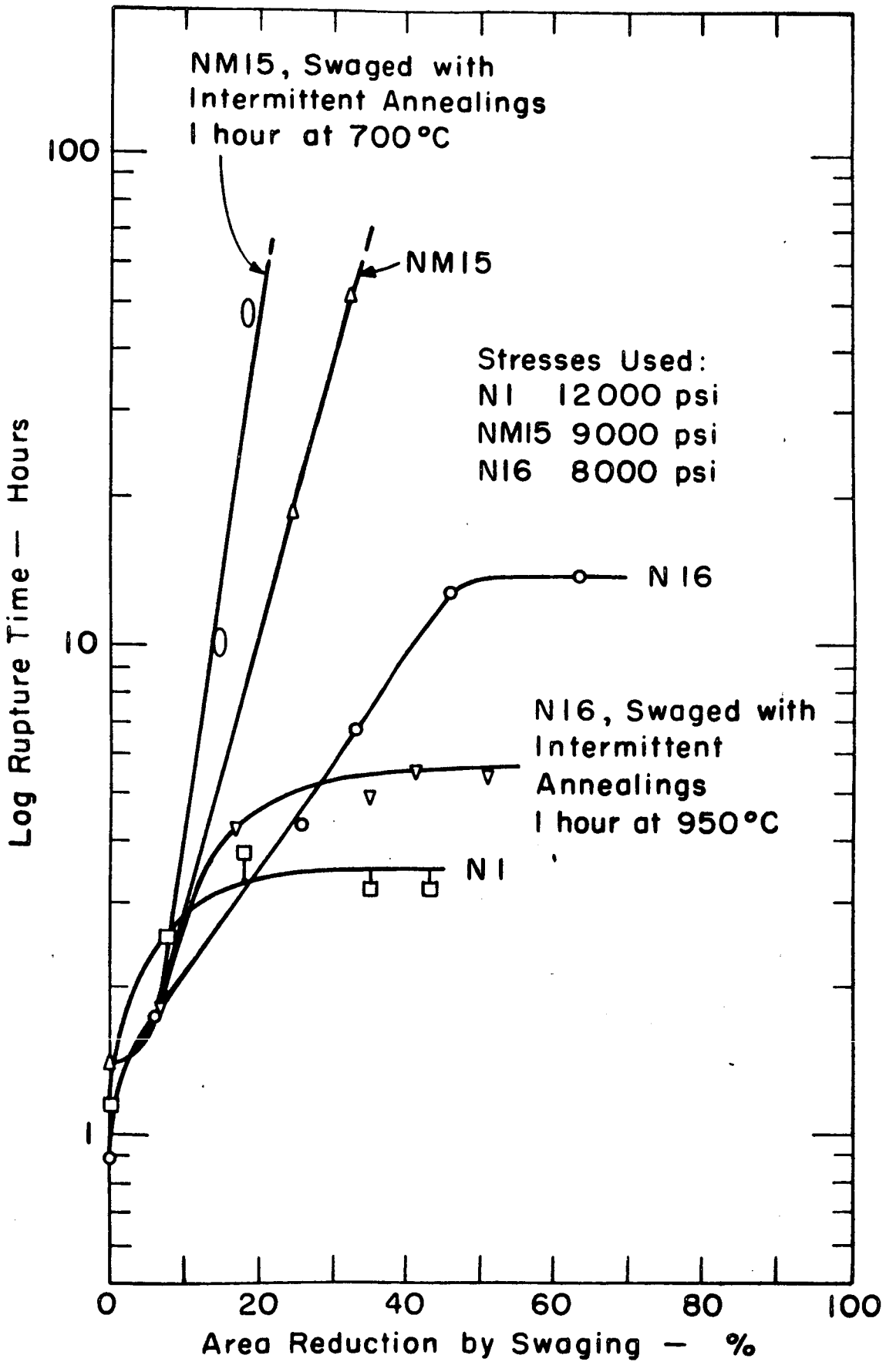

Figure 9. Increase in rupture life with increasing cold swaging, with and without intermittent annealing treatments.

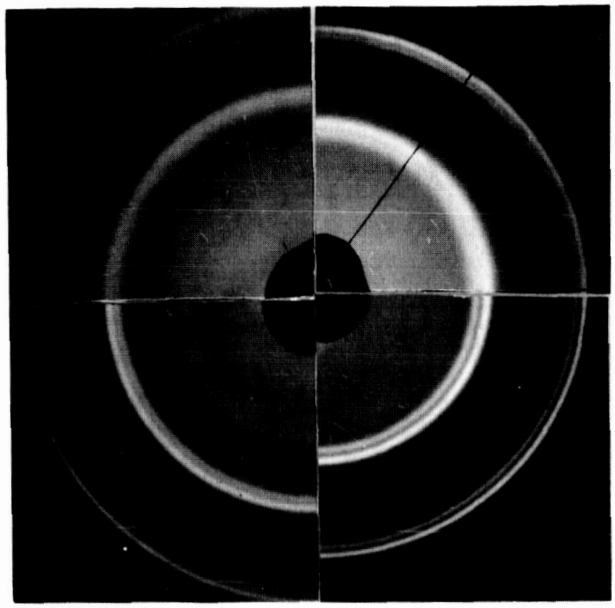

Fig. 10 Pinhole back-reflections of Alloys NM15 and M16.

A. NM15 cold swaged 25%
B. Condition A after 1 hour at 950°C
C. M16 cold swaged 25%
D. Condition C after 1 hour at 700°C

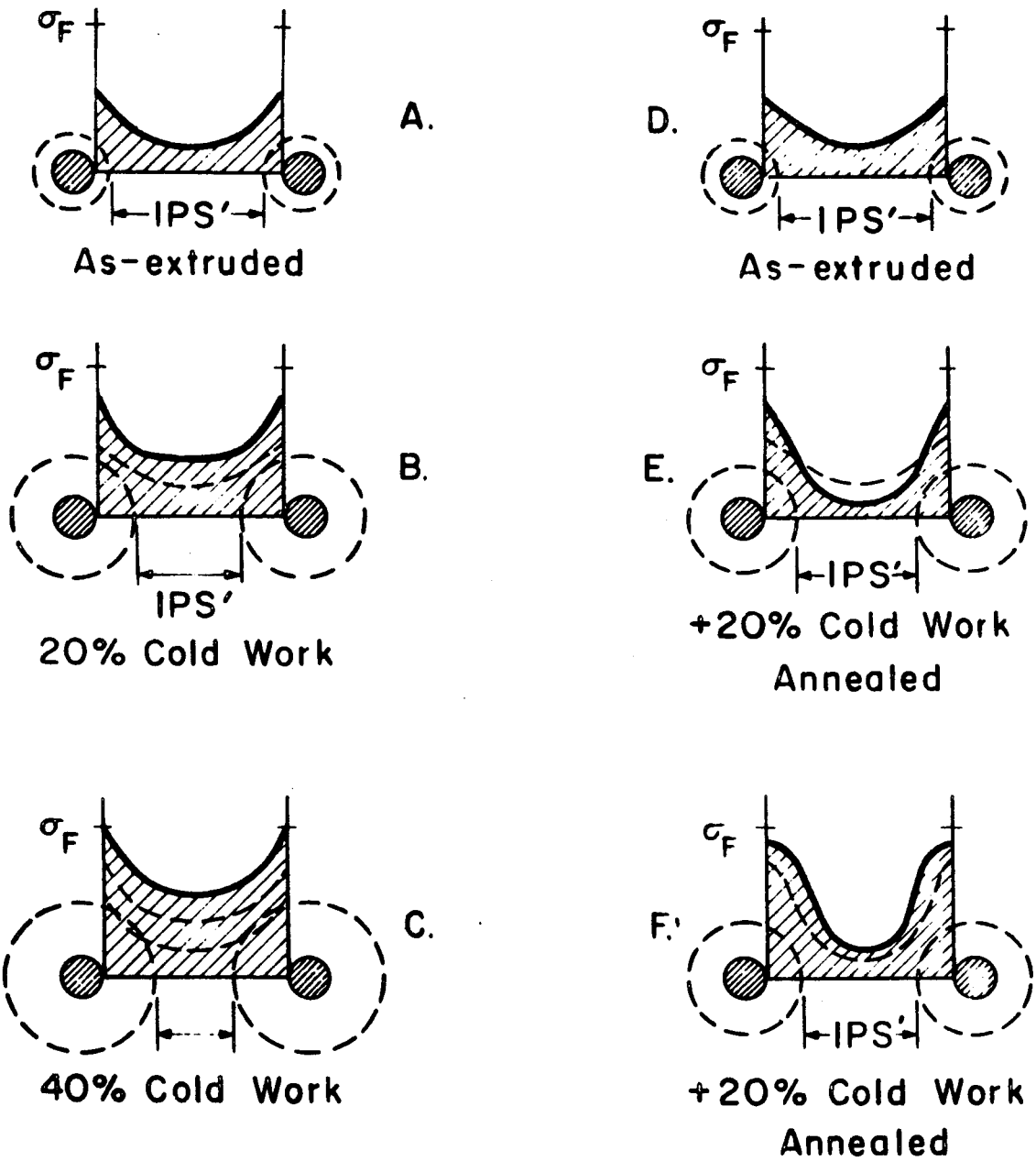

Figure 11. Model of Energy distribution.